IOP Publishing Journal of Physics: Condensed Matter
J. Phys.: Condens. Matter **28** (2016) 425001 (8pp) doi:10.1088/0953-8984/28/42/425001

Impact of orthogonal exchange coupling on magnetic anisotropy in antiferromagnetic oxides/ferromagnetic systems

Piotr Kuświk[1,2], Pedro Lana Gastelois[2,3], Hubert Głowiński[1], Marek Przybylski[2,4] and Jürgen Kirschner[2,5]

[1] Institute of Molecular Physics, Polish Academy of Sciences, 60179 Poznań, Poland
[2] Max-Planck-Institut für Mikrostrukturphysik, 06120 Halle, Germany
[3] Centro de Desenvolvimento da Tecnologia Nuclear, 31270-901 Belo Horizonte, MG, Brazil
[4] Academic Centre for Materials and Nanotechnology and Faculty of Physics and Applied Computer Science, AGH University of Science and Technology, 30-059 Kraków, Poland
[5] Institut für Physik, Martin-Luther-Universität Halle-Wittenberg, 06120 Halle, Germany

E-mail: kuswik@ifmpan.poznan.pl

Received 2 June 2016, revised 4 August 2016
Accepted for publication 10 August 2016
Published 2 September 2016

Abstract

The influence of interface exchange coupling on magnetic anisotropy in the antiferromagnetic oxide/Ni system is investigated. We show how interfacial exchange coupling can be employed not only to pin the magnetization of the ferromagnetic layer but also to support magnetic anisotropy to orient the easy magnetization axis perpendicular to the film plane. The fact that this effect is only observed below the Néel temperature of all investigated antiferromagnetic oxides with significantly different magnetocrystalline anisotropies gives evidence that antiferromagnetic ordering is a source of the additional contribution to the perpendicular effective magnetic anisotropy.

Keywords: perpendicular exchange bias, thin films, perpendicular magnetic anisotropy

(Some figures may appear in colour only in the online journal)

1. Introduction

When antiferromagnetic/ferromagnetic (AFM/FM) bilayers are cooled below the Néel temperature (T_N) of the AFM in an external magnetic field known as the field cooling (FC) procedure, the hysteresis loop of the FM layer exhibits enhanced coercivity (H_C) and a shift along the field axis [1]. This last phenomenon is called the exchange bias field (H_{EB}) and is defined as the shift between the zero field and the center of the displaced hysteresis loop. The enhanced H_C and the presence of H_{EB} occur when the AFM order is established in the presence of the ferromagnetism via the interfacial FM–AFM interaction described by the exchange coupling constant J_{EB}. To explain this phenomenon, several basic models have been proposed. The first is the ideal Meiklejohn–Bean (M&B) model, which overestimates the magnitude of H_{EB} [1]. Later modifications of this model establish a more realistic M&B model, where it was shown that H_{EB} can exist only if $K^{AFM}t_{AFM} > J_{EB}$ (where K^{AFM} and t_{AFM} are the anisotropy constant and the thickness of the antiferromagnetic layer, respectively), however, without enhancement of H_C [2]. It should be noted that in this model it is assumed that the AFM with t_{AFM} is in the single-domain state. Because of that, the variation of H_{EB} with variable t_{AFM} may not be well described, especially for the polycrystalline layer, where t_{AFM} should be expressed by V/A (where V is the volume of the AFM grain with surface area A) [3]. Microscopically, the shift is explained by random field theory [4–6], in which the formation of AFM domains is assumed to be due to interfacial roughness when FC is applied to the FM/AFM system. Various models suggest that spin-flop coupling resulting from the interfacial spins being frustrated [7–9], and/or domain wall pinning resulting from defects [10] at the FM/AFM interface, are the mechanisms responsible for coercivity enhancement. Later on, it was shown that

not only does the interface play an important role in the EB effect but so does the domain state of the granular AFM layer [3, 11–13]. To overcome the interconnection between H_C and H_{EB}, the spin glass (SG) model was introduced [14]. In this model, the AFM interface is divided into two types of AFM spins: frozen-in and rotatable. As a consequence, some interfacial disorder is assumed, described by the conversion factor f, which merges this model with the realistic M&B model. Existence of these two types of spins at the interface was recently proven using the x-ray magnetic circular dichroism (XMCD) technique [15].

The exchange bias effect has been widely investigated in AFM/FM systems, presenting either in-plane or perpendicular magnetic anisotropy (PMA) of the FM layer, because of their potential application in spintronics. Very recent discoveries make the interface exchange coupling even more fascinating because this coupling can change the magnetic easy axis of FM layers from the in-plane to the out-of-plane direction. This change is attributed to the perpendicularly oriented unpinned magnetic moments of the AFM layer at the AFM/FM interface. These observations were made for Mn/Fe systems [16]. However, for the fully compensated AFM surface in AFM/FM bilayers, theoretical work predicts orthogonal coupling between AFM and FM spins [7], which can be a source of uniaxial magnetic anisotropy, and H_{EB} is induced by interfacial defects [9]. Recently, an in-plane spin-reorientation transition driven by perpendicular exchange coupling has been observed experimentally for the ferromagnetic coupled layer with a fully compensated surface of NiO(0 0 1). An example of this is Fe/NiO bilayers grown on an Ag(0 0 1)-stepped surface [17], where the Ni spins are aligned in the sample plane. For another fully compensated surface, CoO(0 0 1), with the in-plane orientation of Co spins, it was found that an $L1_0$-FePt/CoO bilayer with perpendicular magnetic anisotropy of FePt presents robust orthogonal exchange coupling observed up to room temperature (RT) [18]. Furthermore, we have previously demonstrated that such orthogonal exchange coupling introduces a supplementary contribution term to the magnetic anisotropy that supports the perpendicular easy magnetization axis of CoO-coated Ni films [19]. This CoO/Ni/Pd(0 0 1) system also presents perpendicular exchange bias. Very recently, it was also found that PMA can be induced by exchange coupling in a Co/NiO polycrystalline system [20].

In this paper, we investigate the influence of exchange coupling on the magnetic anisotropy of Ni layers grown on Pd(0 0 1) covered with different antiferromagnetic oxides (AFOs) (e.g. CoO, NiO, and CoO/NiO bilayer). In uncovered thin Ni/Pd(0 0 1) films, the perpendicular anisotropy is induced by strong tetragonal distortion caused by the large lattice mismatch between Ni(0 0 1) films and the Pd(0 0 1) substrate. This strong tetragonal distortion is responsible for a large volume contribution to the effective anisotropy [21], which is strong enough to overcome the negative surface contribution and the shape anisotropy of Ni films. Therefore, Ni films present perpendicular anisotropy from 2 to 15 monolayers (MLs). Above this thickness, the film structure is relaxed, and the volume contribution favoring PMA of the Ni film is reduced. As a consequence, the negative surface contribution and the shape anisotropy become dominant and the magnetization of the film is oriented in the sample plane. The magnetic and structural properties of the these films are described in detail in [22]. In the present work, it is demonstrated that the perpendicular magnetic anisotropy of Ni/Pd(0 0 1) films can be enhanced by exchange coupling with different antiferromagnetic cover layers. As an extension to our previous work on Ni/Pd(0 0 1) films covered with CoO [19], we have explored in more detail different combinations of CoO and NiO as the AFM layer. We demonstrate that, at temperatures lower than T_N of the AFOs, in an AFO/Ni system, the exchange coupling favors perpendicular magnetization orientation of the Ni film. This temperature-driven spin-reorientation transition is directly related to the ordering temperature of the AFO layer, which can be controlled by the proper choice of the AFO sublayer and its thickness. Hence, we discuss the role of the AFM anisotropy constant on the perpendicular anisotropy induced by the perpendicular exchange coupling.

2. Experiment

Samples were prepared in a multichamber ultrahigh vacuum system with pressure below 2×10^{-10} mbar during deposition. Pd(0 0 1) crystals were cleaned using cycles of 1 keV Ar ion sputtering and subsequent annealing at ∼900 K. Ni wedge samples were grown using molecular beam epitaxy at RT. The uniform CoO layer was grown in two steps. First, the Ni wedge was covered with a single layer of Co to protect the Ni layer from oxidation. Then, the sample was heated to 380 K and exposed to oxygen for 200 s at a pressure of 7.7×10^{-7} mbar. As a result, 1 ML of CoO was created. In the second step, keeping same the substrate temperature, oxygen pressure, and deposition rate of Co, the first CoO layer was covered with 2 ML of a CoO(0 0 1) overlayer, resulting in a total of 3 ML of CoO. Exactly the same growth conditions were applied to CoO grown directly on Pd(0 0 1) and then covered with a Ni wedge. In addition, one other sample was grown by exposing the Ni layer to oxygen for 200 s at a pressure of 7.7×10^{-7} mbar, before the CoO layer was deposited by applying the same previously mentioned growth procedure.

The epitaxial growth assures a single crystalline structure, which is advantageous for comparison to the polycrystalline structure usually investigated in exchange bias systems. Additionally, growing the film in wedge-shape samples guarantees the same conditions for substrate preparation and for layer deposition, reducing the source of uncontrollable variables, when studying thickness-dependent effects.

The film structures were monitored by low-energy electron diffraction (LEED) and reflection high-energy electron diffraction (RHEED). The LEED patterns, presented in figure 1, were collected using an electron energy of 80 eV. The incident electron beam was oriented perpendicularly to the surface plane. The RHEED patterns were taken along the [1 0 0] direction of the Pd substrate. RHEED intensity oscillations were used to calibrate the evaporation rates.

Magnetic properties were probed using the *in situ* polar and longitudinal magneto-optical Kerr effect (MOKE) with a laser

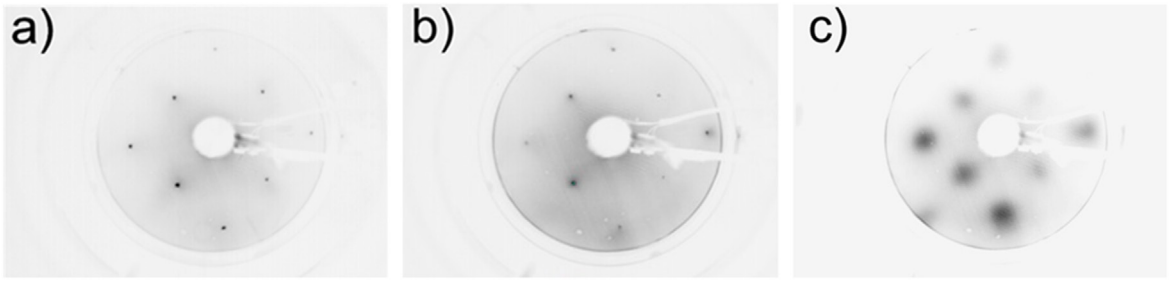

Figure 1. LEED patterns of (a) bare Pd substrate, (b) 6 ML of Ni grown at RT on Pd(0 0 1), and (c) 3 ML of CoO grown at 380 K on top of 6 ML of Ni on Pd(0 0 1). All patterns were measured at RT using an electron energy of 80 eV.

diode (whose wavelength was 670 nm and whose beam diameter was <0.2 mm) at incidence angles of 69° and 30°, respectively. MOKE measurements were performed by applying an external magnetic field up to 0.6 tesla, in a wide temperature range (from RT to $T = 5$ K). Note that MOKE probes the magnetization of the AFM/FM double-layer films via the loops measured for the FM-Ni films, which are affected by the AFM/FM interface coupling.

3. Results

We performed structural analysis of Ni films in the thickness range between 0 and 28 ML grown on Pd(0 0 1) using LEED. For a clean Pd substrate (figure 1(a)) and after deposition of Ni films (figure 1(b)) the LEED patterns exhibited well-defined spots with a cubic (1 × 1) ordered surface, confirming that the Ni film grows epitaxially on the Pd(0 0 1) substrate. RHEED and grazing incidence x-ray diffraction (GIXRD) experiments revealed that the epitaxial Ni films are initially strongly tetragonally distorted for thin film; however, it relaxes as the film thickness increases [19]. For thicknesses >15 ML the Ni films are almost completely relaxed, presenting the lattice parameters close to the Ni bulk values [22].

After deposition of 3 ML CoO on top of Ni, the LEED patterns were used to monitor the quality and crystallographic orientation of the CoO layer (figure 1(c)). The LEED diffraction spots from the CoO layer are strongly diffused compared to the Ni spots (figure 1(b)). This probably is related to the charging of the sample surface during the measurements, rather than to the crystallinity of the layer [23]. However, the position of the spots clearly indicates that CoO grows epitaxially with the (0 0 1) surface plane. Moreover, from our previous GIXRD measurements [19], we know that the CoO has a rock-salt-like structure with an in-plane lattice constant of 4.15(2) Å and, after covering the Ni layer with CoO, the lattice parameters of the Ni films remain unchanged. When the CoO is grown directly on the Pd(0 0 1) substrate, we expected similar (0 0 1) growth to what was observed for CoO/Ir(0 0 1) [24].

The description of the magnetic anisotropy of Ni films grown on Pd(0 0 1) is an important starting point for understanding the magnetic interaction between Ni and AFOs in the AFO/Ni bilayer. Ni films epitaxially grown on Pd(0 0 1) exhibit a perpendicular easy magnetization axis from the thickness of 2 ML (only at 5 K) up to 15 ML (at RT) owing

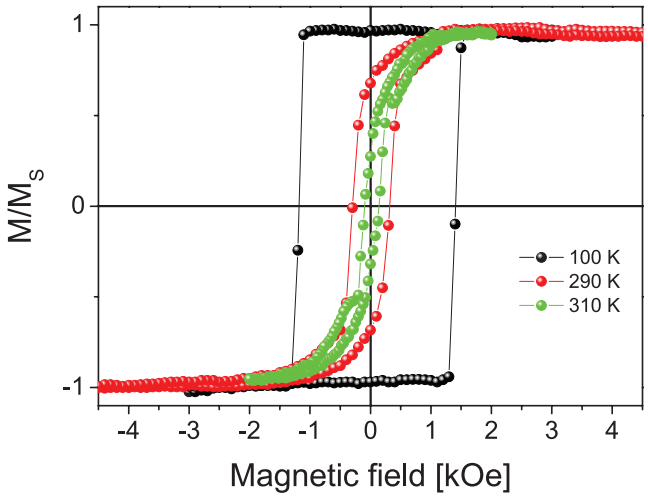

Figure 2. PMOKE hysteresis loops for CoO/Ni(23 ML)/Pd(0 0 1) measured at different temperatures after FC procedure (at −3.8 kOe).

to tetragonal distortion [25]. Around this thickness, the Ni/Pd(0 0 1) system undergoes a spin-reorientation transition (SRT) and, for thicker layers, presents hysteresis loops characteristic for in-plane anisotropy (as shown for a 23 ML-thick Ni film at RT and at 5 K in [19]). Its magnetic properties are discussed and reported in more detail elsewhere [22].

In our previous investigation [19], we found that, after deposition of 3 MLs of CoO on top of Ni/Pd(0 0 1) and after field cooling (from 450 to 5 K in $H \perp = -3.8$ kOe), the CoO drives the Ni magnetization to be oriented perpendicularly to the sample plane. This effect was only observed below the Néel temperature of the CoO. In this paper, to understand the effect of the covering CoO on magnetic anisotropy of the Ni film, we focus on investigating the effect of exchange coupling and its temperature dependence on one particular thickness (23 ML) of Ni. When characterizing the CoO/Ni/Pd(0 0 1) system by PMOKE, there are a few important parameters to be considered from the hysteresis loops (figure 2): squareness of the hysteresis loop (M_R/M_S), where M_S and M_R are the Kerr ellipticity values at saturation and at remanence, respectively, the exchange bias field (H_{EB}), and coercivity (H_C). M_R/M_S, H_{EB}, and H_C as functions of the temperature determined by the polar MOKE for CoO(3 ML)/Ni(23 ML)/Pd(0 0 1) are shown in figures 3(a)–(c), respectively. Based on these results, four distinct ranges of temperature related to different magnetic properties of the Ni film covered with CoO can be distinguished:

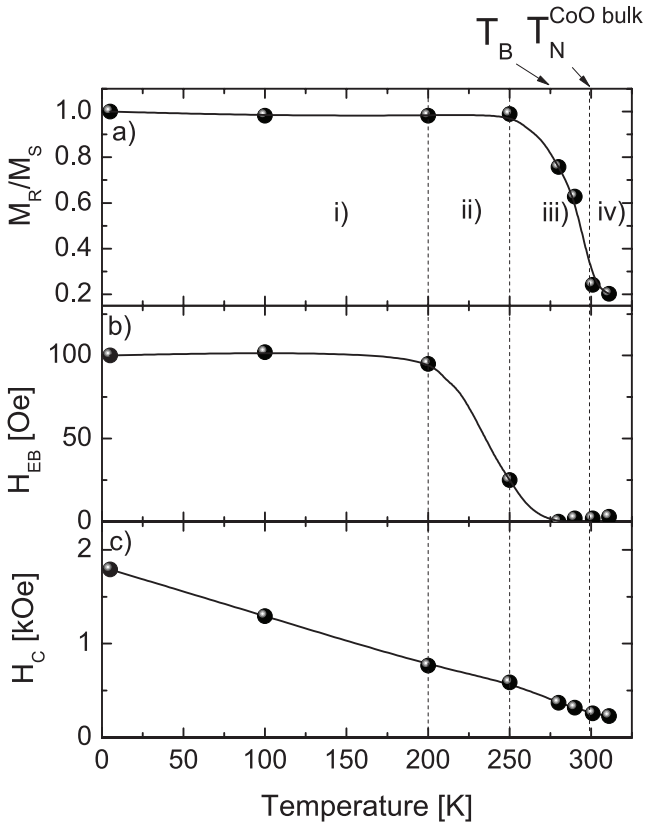

Figure 3. (a) Squareness of the PMOKE loops, (b) exchange bias fields, and (c) coercivities plotted versus temperature for 23 ML of Ni film covered with 3 ML of CoO, after FC (at −3.8 kOe). All lines are guides to the eye. T_B and T_N denote the blocking and Néel temperatures, respectively.

(i) $T \lesssim 200$ K: $M_R/M_S = 1$, rectangular polar hysteresis loops are measured, Ni is characterized by strong PMA with almost constant $H_{EB} = 100$ Oe owing to orthogonal interface exchange coupling [19].
(ii) $200 \lesssim T \lesssim 250$ K: $M_R/M_S = 1$, the Ni film has strong PMA, but the exchange bias is strongly reduced.
(iii) $250 \lesssim T \lesssim 300$ K: M_R/M_S decreases, which indicates that the Ni layer undergoes an SRT from perpendicular to in-plane anisotropy, whereas $H_{EB} \cong 0$
(iv) $T \gtrsim 300$ K: $M_R/M_S \ll 1$ hysteresis loops show that the effective anisotropy of Ni film is in the sample plane.

To verify whether the temperature at which the perpendicular anisotropy starts to decrease is related to the antiferromagnetic state of CoO, we introduce to the CoO/Ni system an additional NiO layer to change the Néel temperature of the AFM layer. The Néel temperature of bulk CoO is 293 K [26] and can be even lower in CoO ultrathin films [26, 27]. To change T_N of the coupled AFM layer, the topmost atomic layers of Ni were intentionally oxidized [28, 29] and then covered with another 3 ML of CoO. Additionally, before deposition of the CoO layer, PMOKE measurements were also performed for NiO/Ni/Pd(0 0 1). The thickness of NiO is estimated from the decrease of the Kerr signal at saturation to be 2–3 ML. From figure 4(a), it is clearly seen that for CoO/NiO/Ni/Pd(0 0 1) perpendicular magnetization of the Ni film is restored in the Ni thickness range of 17–25 ML even at RT. This is attributed to the antiferromagnetic state of CoO/NiO, which is above RT. At RT, H_{EB} is close to zero (figure 4(b)) and the interface exchange coupling in this case is only manifested by the enhanced H_C (figure 4(c)). In the NiO/Ni/Pd(0 0 1) system, at RT, Ni has in-plane anisotropy and the SRT was unchanged compared to an uncovered Ni film (figure 4(a)). Moreover, there is no enhancement of H_C and $H_{EB} = 0$ (figures 4(b) and (c)), indicating that T_N of the 2–3 ML NiO is below RT. Note that T_N strongly depends on the thickness of the NiO(0 0 1) layer. It was previously demonstrated, by x-ray magnetic linear dichroism (XMLD) measurements, that the ordering temperatures of 5, 10, and 20 ML of NiO are 300, 430, and 470 K, respectively [30]. According to these data, we expect that, for 2–3 ML of NiO, T_N is lower than RT. To verify whether this NiO layer has AFM ordering at lower temperature we have measured the hysteresis loops for this system also at 5 K. Based on the results for CoO and CoO/NiO, we have expected an additional contribution, which induced PMA of the Ni layer. Indeed, the SRT is shifted to a thicker Ni layer, extending the thickness range, where PMA of the Ni film is observed (figure 4(d)), similar to what was found for CoO/Ni and CoO/NiO/Ni. Moreover, at this temperature, we observed shifts of the hysteresis loops (figure 4(e)) and enhanced coercivity (figure 4(f)), which confirmed the AFM ordering of 2–3 ML of NiO.

To investigate the role of the interlayer coupling between CoO and Ni, we reversed the sequence of the layer deposition of growing the Ni film on top of the CoO layer that was first grown on Pd(0 0 1). This experiment has shown that at RT the SRT occurs around a Ni layer thickness of 15–17 ML, as identically observed in the CoO/Ni/Pd(0 0 1) system. After FC with an applied magnetic field perpendicular to the sample plane, at low temperature this system exhibits PMA behavior similar to that of CoO/Ni/Pd(0 0 1) (figure 5(a)), however, with a much higher H_{EB} (figure 5(b)). The detailed analysis for this system was performed at 100 K, because for low thicknesses at 5 K we expect a large coercivity. (Note that loops presenting too large a coercivity could not be measured given the largest magnetic field we can apply.) At 100 K the measured hysteresis loops were rectangular ($M_R/M_S = 1$) for all thicknesses, indicating that the Ni layer in this thickness range has strong PMA. The loops are clearly shifted along the field axis by perpendicular exchange coupling between Ni and CoO. The value of H_{EB} is much higher than that for the CoO/Ni/Pd(0 0 1) system, which is probably related to the higher roughness at the AFM/FM interface. Therefore, for this sample we decided to verify the role of the magnetization direction of Ni during the field cooling procedure in inducing the PMA of this film. We performed cooling with different magnetic field orientations: perpendicular (FC$\perp$) and in plane (FC$\parallel$) as well as zero-field cooling (ZFC). At 100 K the PMA of the Ni film is present for all cooling procedures, indicating that the direction of the Ni film during field cooling does not significantly influence the effective anisotropy (figure 5(a)) nor coercivity of the Ni layer (figure 5(c)). Only H_{EB} strongly depends on this cooling procedure (figure 5(b)). For FC$\perp$ and ZFC, H_{EB} is reciprocally proportional to the thickness of the FM film [31]. For a thickness in which the Ni film has PMA without coupling (range $*$,

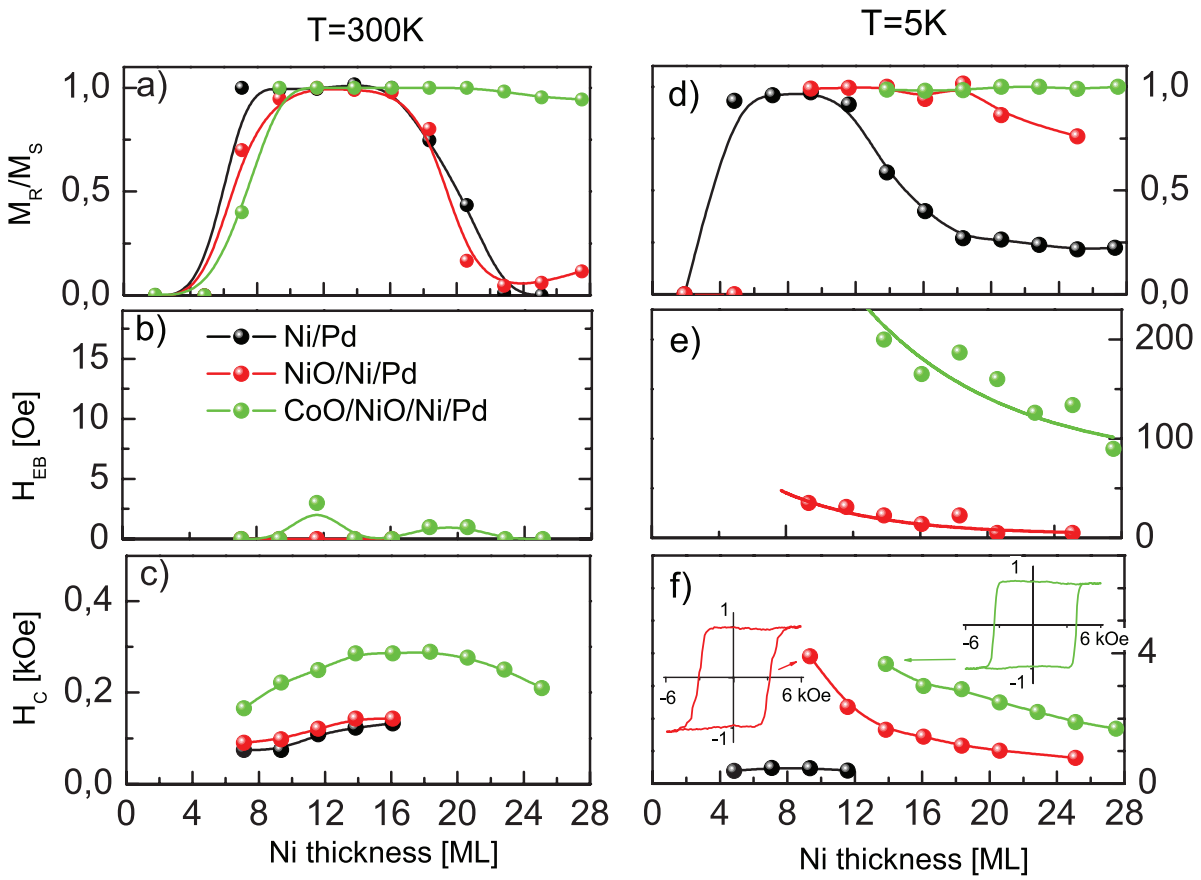

Figure 4. ((a) and (d)) Squareness of the hysteresis loops, ((b) and (e)) exchange bias field, and ((c) and (f)) coercivity plotted versus Ni film thickness, after oxidation (2–3 ML of NiO), and after additional covering with 3 ML of CoO. All cases are measured at ((a)–(c)) RT and at ((d)–(f)) 5 K. Covering with CoO/NiO induces perpendicular magnetization of thick Ni films, even at RT. All lines are guides to the eye. Insert in panel (f) presents the PMOKE hysteresis loop measured for the NiO/Ni(9 ML)/Pd(0 0 1) and CoO/NiO/Ni(14 ML)/Pd(0 0 1) at 5 K.

figure 5(b)), H_{EB} is exactly the same as for FC⊥ and ZFC. This shows that for 10–14 ML of the Ni film FC⊥ is not needed to induce the exchange bias field since the FM film is saturated along the easy magnetization axis, which is equivalent to a saturation magnetic field applied perpendicular to the sample plane. However, a difference between FC⊥ and ZFC appears for higher Ni thickness (range $**$), where for $H = 0$ the Ni film has a nonzero in-plane magnetization component (figure 5(b)). Thus, for FC⊥ the perpendicular field $H = -4000$ Oe applied during the FC aligned the Ni spins perpendicularly to the sample plane. As a result, for ZFC H_{EB} is smaller than for FC⊥. Surprisingly, after FC‖ is applied, almost no exchange field was observed either for low or high Ni thickness (figure 5(b)), while the PMA still exists.

4. Discussion

4.1. Orthogonal exchange coupling as a source of PMA of the Ni layer in the AFO/Ni/Pd(0 0 1) system

The stepped deposition, described in the experiment section, was used to achieve an in-plane-compressed CoO(0 0 1) surface exhibiting in-plane orientation of the spin axis [32]. Since the lattice mismatch between CoO and Ni/Pd is large (∼9.5%), the growth of 3 ML of CoO is not strictly pseudomorphic to the Ni/Pd(0 0 1) substrate. Nevertheless, there is still a residual, in-plane compressive strain and thus a tetragonal distortion in the CoO overlayer. The tetragonal distortion can lead to a modified electronic structure of CoO and, in the case of compressive strain forces, in-plane orientation of the spin axis [32, 33]. Indeed, in our previous XMLD experiments [19], we confirmed that in the CoO/Ni/Pd(0 0 1) system, the CoO spin axis lies in the sample plane because of the tetragonal distortion. Very recent XMLD experiments on NiO/CoO grown on MgO(0 0 1) [34, 35] show that the orientation of magnetic moments in very thin NiO films follows the CoO spins because of a strong exchange interaction at the interface and the small magnetocrystalline anisotropy constant of NiO, which for very thin NiO can be even smaller [30]. Based on the results from [34], we assumed that, in our CoO/NiO system, the spin axis lies in the sample plane, as was found for CoO/Ni [19]. It should be noted that the preferred orientation of spins in NiO grown on Ag(1 0 0) is found to be in the sample plane owing to compressive strain [36], similarly as was found for CoO/Ag(0 0 1) [32].

The reported magneto-optical results for the covered Ni-wedge/Pd(0 0 1) with AFOs (CoO, NiO, and CoO/NiO) indicate that the Ni film exhibits a perpendicular easy magnetization axis in the thickness range of 17–25 ML for all investigated systems, however, at different temperature ranges

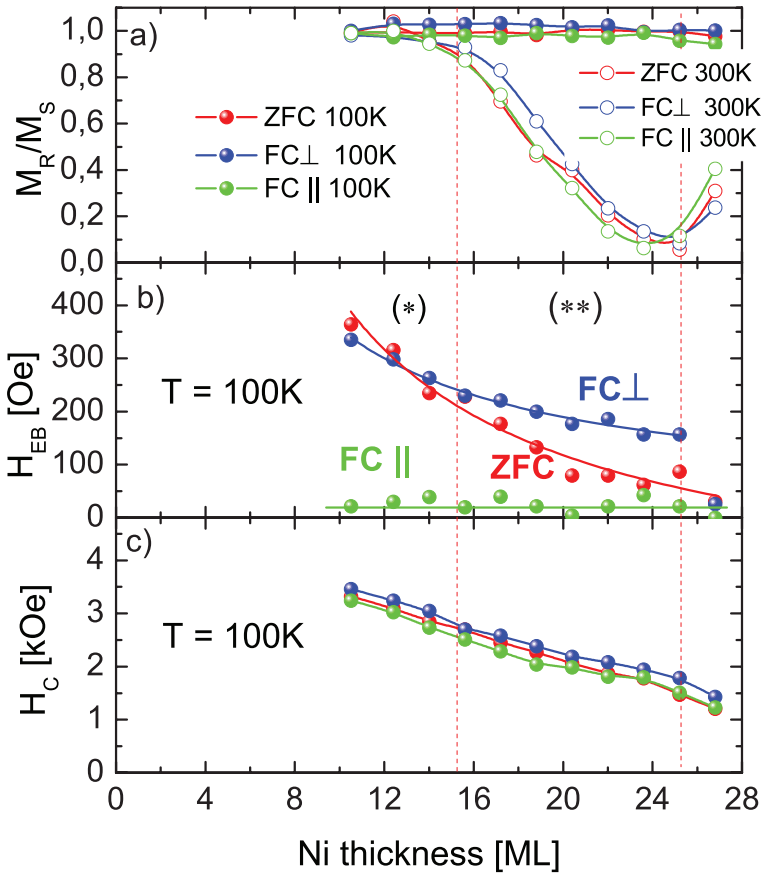

Figure 5. (a) Squareness of the hysteresis loops, (b) exchange bias fields, and (c) coercivity plotted versus thickness of Ni on top of 3 ML of CoO on Pd(0 0 1) measured at RT and at 100 K after different field cooling procedures. FC⊥ and FC‖ indicate perpendicular and in-plane orientation of the magnetic field, respectively. All lines are guides to the eye.

(figures 3(a) and 4(a) and (d)). In addition to the perpendicular magnetic anisotropy of the Ni layer, this system also presents large coercivity and an exchange bias effect (figures 4(e) and (f)). This temperature-driven spin-reorientation transition from the out-of-plane to in-plane direction is correlated with the ordering temperature of AFO films. Since the interface exchange coupling supports perpendicular magnetization of the Ni film, and assuming that the spins of CoO, NiO, and NiO/CoO lie in the sample plane, we postulate that, for all investigated AFOs, orthogonal interface exchange coupling exists.

4.2. Temperature investigations indicating the mechanism responsible for PMA of the Ni film sandwiched between Pd(0 0 1) and AFO

In figure 3 we distinguish four distinct ranges of temperature, where the Ni film in contact with CoO has different magnetic properties. Because the exchange coupling energy, which favors perpendicular anisotropy, is strong enough ($J = 0.183$ erg cm^{-2}) [19], the easy magnetization axis is oriented perpendicular to the sample plane up to ~200 K with almost constant $H_{EB} = 100$ Oe (range i). Above 200 K (range ii), the exchange bias is strongly reduced, surprisingly keeping the PMA of Ni layer. When the temperature reaches 270 K (range iii), H_{EB} becomes zero, indicating that the blocking temperature ($T_B = 270$ K) is smaller than the ordering temperature of CoO ($T_N = 293$ K). For very thin antiferromagnetic films, this difference between T_B and T_N is well known [31] and is related to the reduced K^{AFM} [37]. In M&B and SG models it is assumed that, for a constant t_{AFM}, the exchange bias can only exist above the critical value of $K^{AFM} > K^{AFM}_{crit}$, where K^{AFM}_{crit} is proportional to the exchange coupling energy and conversion factor describing the fraction order at the interface [31]. Because for AFOs such as CoO and NiO [38] K^{AFM} decreases with temperature as $K^{AFM} \propto (1 - T/T_N)^2$, at a certain temperature $T = T_B$, the condition $K^{AFM} > K^{AFM}_{crit}$ cannot be fulfilled and the AFM spins can follow the FM spins during the reversal process [14, 31]. As a consequence, $H_{EB} = 0$ and only enhancement of H_C is observed.

This explanation can be applied to our system, where below 200 K (range i) K^{CoO} is high enough to induce both the exchange bias effect and large H_C (figures 3(b) and (c)). However, approaching the blocking temperature (range ii and iii), K^{CoO} becomes weaker, causing strong reduction of H_{EB}. Finally, at $T = T_B$, interface exchange coupling is manifested only by the enhancement of H_C, whereas $H_{EB} = 0$ because $K^{CoO} < K^{CoO}_{crit}$. From data presented in figure 3 it is clear that, at T_B, the additional contribution to magnetic anisotropy favoring the PMA of the Ni film still exists ($M_R/M_S = 0.75$), suggesting that the exchange bias effect and thus unidirectional anisotropy induced by the AFM–FM interaction at the

interface may not be responsible for perpendicular magnetization of 23 ML of the Ni film. We found that the contribution favoring the PMA of the Ni film steadily decreases with increasing temperature, from 250 to 300 K (range iii), because in this temperature range (between T_B and T_N of our CoO layer) $K^{CoO} < K^{CoO}_{crit}$, the $H_{EB} = 0$ and the interface exchange coupling is indicated only by enhancement of H_C. This suggest that, a certain contribution to the PMA of Ni film exists, even for a significantly reduced value of K^{CoO}, which can be smaller than K^{CoO}_{crit}. Only above T_N when the AFM layer is in the paramagnetic state ($K^{CoO} = 0$) (range iv) is the magnetic anisotropy of Ni almost unchanged if compared to uncovered Ni films grown on Pd(0 0 1).

To prove that the ordering temperature rather than K^{AFM} plays an important role in establishing PMA of Ni film, experiments with different AFO layers (NiO and CoO/NiO) were performed. Note that $K^{NiO} = 3.3 \times 10^2$ erg cm^{-3} is much smaller than $K^{CoO} = 2 \times 10^5$ erg cm^{-3} [39]. However, this huge difference in the anisotropy of CoO and NiO bilayers does not affect the range of Ni thickness at 5 K, where PMA of Ni was found (figure 4(d)), similarly as we found for a CoO/NiO layer on top of Ni/Pd(0 0 1). Important is the fact that, for these three AFOs, T_N changes drastically. Oxidation before deposition of CoO results in remarkably increased Néel temperature since the Néel temperature of thick NiO is equal to 525 K [40, 41]. Moreover, in $[NiO/CoO]_N$ superlattices, T_N enhancement has been confirmed by neutron diffraction and heat capacity measurements [39, 42]. Also, XMLD measurements confirm that the exchange coupling between CoO and NiO can enhance T_N of the CoO layer, which is much higher than that of a CoO single layer. Because in our system the thickness of NiO is estimated to be of 2–3 ML, we expect, according to data from [30], that in the NiO/Ni/Pd(0 0 1) system T_N is below RT. This difference of T_N of AFOs is well correlated with temperatures where the coupling favors the PMA of the Ni film in our experiments. Since the exchange coupling is much stronger than the product of effective in-plane anisotropy and the Ni film of the thickness just above SRT, the magnetization of the AFO/Ni system follows the coupling direction; i.e. it tends to be oriented perpendicular to the sample plane. When temperature increases above T_N of AFO, magnetization of the paramagnetic-AFO/Ni bilayer rotates toward the sample plane as it was before covering with AFO.

Therefore, in all three cases of CoO/NiO, CoO, and NiO grown on Ni/Pd(0 0 1) the additional contribution to the perpendicular anisotropy was present, however, at a different temperature range. This temperature range was related to the antiferromagnetic state of the particular layer but is not correlated to the range of temperature where H_{EB} was observed. It is known that, in AFM/FM systems, exchange biasing is strongly related to the anisotropy of the AFM layers, as was demonstrated experimentally by the fact that higher bias fields are obtained for higher anisotropy materials [39]. Indeed, the exchange bias field at 5 K for Ni/Pd(0 0 1) covered by NiO is much smaller than for that covered by CoO/NiO (figure 4(e)), which we correlated with the smaller anisotropy constant of NiO, as was mentioned earlier. Despite very small H_{EB}, the interface exchange coupling is manifested by the enhanced H_C. Therefore, it seems that the ordering of the AFM state plays the most important role in introducing the additional perpendicular contribution to the effective anisotropy of Ni film. Moreover, the obtained data for different FC procedures reveal that, after FC$\parallel$ is applied, almost no exchange field was observed either for low or high Ni thickness (figure 5(b)). Nevertheless, PMA of Ni was observed at 100 K, as was similarly shown for FC$\perp$ and ZFC, which supports the conclusion that exchange biasing is not required to force FM spins to be magnetized perpendicular to the sample plane.

5. Summary

In summary, we studied the impact of interface exchange coupling on perpendicular magnetic anisotropy and perpendicular exchange bias in antiferromagnetic oxides (CoO, NiO, and CoO/NiO bilayer)/ferromagnetic-Ni bilayers. We found that the interlayer exchange coupling between investigated antiferromagnetic oxides and ferromagnetic Ni films forces the Ni film to be magnetized perpendicular to the sample plane, however, only below the ordering temperature of antiferromagnetic oxides. This temperature-driven magnetization reorientation from perpendicular to in-plane direction at well-defined temperature can be used as temperature sensors in magnetoresistive spin valve systems. Moreover, the temperature range where this effect occurs and the value of the exchange bias can be tuned by proper choice of AFM thickness or composition, making this phenomenon promising for future applications.

Acknowledgments

PLG and PK acknowledge support from the Max Planck Institute, Halle, during their scientific visit and technical support from W Greie and H Menge. PK also acknowledges support from the National Science Centre, Poland, under SONATA-BIS funding UMO-2015/18/E/ST3/00557.

References

[1] Meiklejohn W H and Bean C P 1956 *Phys. Rev.* **102** 1413–4
[2] Meiklejohn W H 1962 *J. Appl. Phys.* **33** 1328–35
[3] Harres A and Geshev J 2012 *J. Phys.: Condens. Matter* **24** 326004
[4] Malozemoff A P 1987 *Phys. Rev.* B **35** 3679–82
[5] Malozemoff A P 1988 *Phys. Rev.* B **37** 7673–9
[6] Malozemoff A P 1988 *J. Appl. Phys.* **63** 3874–9
[7] Koon N C 1997 *Phys. Rev. Lett.* **78** 4865–8
[8] Suess D, Kirschner M, Schrefl T, Fidler J, Stamps R L and Kim J-V 2003 *Phys. Rev.* B **67** 054419
[9] Schulthess T C and Butler W H 1998 *Phys. Rev. Lett.* **81** 4516–9
[10] Nogués J and Schuller I K 1999 *J. Magn. Magn. Mater.* **192** 203–32
[11] O'Grady K, Fernandez-Outon L E and Vallejo-Fernandez G 2010 *J. Magn. Magn. Mater.* **322** 883–99

[12] Keller J, Miltényi P, Beschoten B, Güntherodt G, Nowak U and Usadel K D 2002 *Phys. Rev.* B **66** 014431
[13] Nowak U, Misra A and Usadel K D 2001 *J. Appl. Phys.* **89** 7269
[14] Radu F, Westphalen A, Theis-Bröhl K and Zabel H 2006 *J. Phys.: Condens. Matter* **18** L29
[15] Wu J, Park J S, Kim W, Arenholz E, Liberati M, Scholl A, Wu Y Z, Hwang C and Qiu Z Q 2010 *Phys. Rev. Lett.* **104** 217204
[16] Wang B-Y, Hong J-Y, Yang K-H O, Chan Y-L, Wei D-H, Lin H-J and Lin M-T 2013 *Phys. Rev. Lett.* **110** 117203
[17] Li J, Przybylski M, Yildiz F, Fu X L and Wu Y Z 2011 *Phys. Rev.* B **83** 094436
[18] Lamirand A D, Soares M M, Ramos A Y, Tolentino H C N, De Santis M, Cezar J C, de Siervo A and Jamet M 2013 *Phys. Rev.* B **88** 140401
[19] Kuświk P, Gastelois P L, Soares M M, Tolentino H C N, De Santis M, Ramos A Y, Lamirand A D, Przybylski M and Kirschner J 2015 *Phys. Rev.* B **91** 134413
[20] Kuświk P, Szymański B, Anastaziak B, Matczak M, Urbaniak M, Ehresmann A and Stobiecki F 2016 *J. Appl. Phys.* **119** 215307
[21] Hjortstam O, Baberschke K, Wills J M, Johansson B and Eriksson O 1997 *Phys. Rev.* B **55** 15026–32
[22] Gastelois P L, Kuświk P, Martins M D, Lamirand A, De-Santis M, Tolentino H C N, Macedo W A A, Przybylski M and Kirschner J 2016 *Phys. Rev.* B submitted
[23] Młyńczak E, Matlak B, Kozioł-Rachwał A, Gurgul J, Spiridis N and Korecki J 2013 *Phys. Rev.* B **88** 085442
[24] Gubo M, Ebensperger C, Meyer W, Hammer K, Heinz L, Mittendorfer F and Redinger J 2012 *Phys. Rev. Lett.* **108** 066101
[25] Winkelmann A, Przybylski M, Luo F, Shi Y S and Barthel J 2006 *Phys. Rev. Lett.* **96** 257205
[26] Ambrose T and Chien C L 1996 *Phys. Rev. Lett.* **76** 1743–6
[27] Maat S, Takano K, Parkin S S P and Fullerton E E 2001 *Phys. Rev. Lett.* **87** 087202
[28] Pan W, Shih Y-T, Lee K-L, Shen W-H, Tsa C-W, We D-H, Chan Y-L and Chang H-C 2012 *J. Appl. Phys.* **111** 07C113
[29] Pappas S D, Kapaklis V, Delimitis A, Jonsson P E, Papaioannou E Th, Poulopoulos P, Fumagalli P, Trachylis D, Velgakis M J and Politis C 2012 *J. Appl. Phys.* **112** 053918
[30] Alders D, Tjeng L H, Voogt F C, Hibma T, Sawatzky G A, Chen C T, Vogel J, Sacchi M and Iacobucci S 1998 *Phys. Rev.* B **57** 11623–31
[31] Radu F and Zabel H 2008 *Magnetic Heterostructures* vol 227 ed H Zabel and S D Bader (Berlin: Springer)
[32] Csiszar S I, Haverkort M W, Hu Z, Tanaka A, Hsieh H H, Lin H-J, Chen C T, Hibma T and Tjeng L H 2005 *Phys. Rev. Lett.* **95** 187205
[33] Boussendel A, Baadji N, Haroun A, Dreyssé H and Alouani M 2010 *Phys. Rev.* B **81** 184432
[34] Zhu J *et al* 2014 *Phys. Rev.* B **90** 054403
[35] Li Q *et al* 2016 *Sci. Rep.* **6** 22355
[36] Altieri S, Finazzi M, Hsieh H H, Lin H J, Chen C T, Hibma T, Valeri S and Sawatzky G A 2003 *Phys. Rev. Lett.* **91** 137201
[37] Duo L, Finazzi M and Ciccacci F (ed) 2010 *Magnetic Properties of Antiferromagnentic Oxide Materials* (New York: Wiley)
[38] Carey M J and Berkowitz A E 1992 *Appl. Phys. Lett.* **60** 3060
[39] Carey M J and Berkowitz A E 1993 *J. Appl. Phys.* **73** 6892–7
[40] Tolentino H C N, De Santis M, Tonnerre J-M, Ramos A Y, Langlais V, Grenier S and Bailly A 2009 *Braz. J. Phys.* **39** 150–5
[41] Tonnerre J M, De Santis M, Grenier S, Tolentino H C N, Langlais V, Bontempi E, Garcia-Fernández M and Staub U 2008 *Phys. Rev. Lett.* **100** 157202
[42] Abarra E N, Takano K, Hellman F and Berkowitz A E 1996 *Phys. Rev. Lett.* **77** 3451–4